

## Synthesis, characterization and antibacterial property of Ag/mesoporous CeO<sub>2</sub> nanocomposite material

LU Xiao-wang<sup>1,2</sup>, QIAN Jun-chao<sup>3</sup>, CHEN Feng<sup>3</sup>, LI Xia-zhang<sup>1</sup>, CHEN Zhi-gang<sup>4</sup>

1. School of Materials Science and Engineering, Changzhou University, Changzhou 213164, China;
2. Key laboratory of Advanced Metallic Materials of Changzhou City, Changzhou 213164, China;
3. School of Materials Science and Engineering, Jiangsu University, Zhenjiang 212013, China;
4. School of Chemistry and Bioengineering, Suzhou University of Science and Technology, Suzhou 215011, China

Received 13 June 2011; accepted 30 September 2011

**Abstract:** Mesoporous CeO<sub>2</sub> with high specific surface area was synthesized using a modified evaporation-induced self-assembly (EISA) method, and a series of different amounts of Ag were loaded to this mesoporous CeO<sub>2</sub> by a modified ethylene glycol reduction route. The samples were characterized by powder X-ray diffraction (XRD), transmission electron microscopy (TEM), energy-dispersive spectrometry (EDS), nitrogen adsorption-desorption, Brunauer–Emmett–Teller (BET) and Barrett–Joyner–Halenda (BJH) methods. The mesoporous CeO<sub>2</sub> structure with different proportions of silver nanoparticles and its antibacterial activity were adequately studied, confirming that obtained novel materials show a good antibacterial effect.

**Key words:** CeO<sub>2</sub>; mesoporous; silver nanoparticle; antibacterial activity

### 1 Introduction

CeO<sub>2</sub> is an important rare earth oxide and has potential applications in areas including catalysis sorption [1,2], polishing agents [3,4], photonic and electronic devices [5–7], gas sensing [8] and solid oxide fuel cells (SOFC) [9,10]. Many metallic and non-metallic elements have been tried, in the past, to be implanted into ceria to improve its catalytic activity [11,12], but few papers concerned with the antibacterial property of nanoparticles implanted in the ceria. Generally, the properties of ceria could be improved from two aspects, structural modification and element decoration.

To achieve higher specific surface area desirable for better applications, several efforts have been made to fabricate mesoporous CeO<sub>2</sub>. Mesoporous CeO<sub>2</sub> is of extremely high surface activity and well oxygen storage capacity due to its porous structure, which can adsorb various ions easily in its pores and on its surfaces. Recently, CORMA et al [13] have synthesized mesostructured CeO<sub>2</sub> materials using CeO<sub>2</sub> nanoparticles as starting materials and a EO<sub>20</sub>PO<sub>70</sub>EO<sub>20</sub> triblock copolymer as the soft template. ROSSINYOL et al [14]

have recently applied SBA–15 and KIT–6 mesoporous silica as the hard template to synthesizing mesoporous ceria.

In order to further improve the properties of CeO<sub>2</sub>, various metal nanoparticles on CeO<sub>2</sub> support were used, such as Pt, Rh, Ru, Au and Ag [15–20]. Silver is known to have a wide antibacterial spectrum and relatively high safety. When silver was supported onto inorganic carrier and released from the surface slowly by design, it acted as inorganic disinfectant, which is superior in terms of safety, durability and heat resistance [21,22]. Herein, the synthesis of mesoporous CeO<sub>2</sub> using CH<sub>3</sub>(CH<sub>2</sub>)<sub>15</sub>N(CH<sub>3</sub>)<sub>3</sub>Br as a soft temple to support the different amounts of Ag on them was reported, the antibacterial activity of the samples was investigated.

### 2 Experimental

#### 2.1 Preparation of mesoporous CeO<sub>2</sub>

Typically, 0.005 mol of cetyltrimethylammonium bromide (CH<sub>3</sub>(CH<sub>2</sub>)<sub>15</sub>N(CH<sub>3</sub>)<sub>3</sub>Br, referred as CTAB, SCRC) was first dissolved in a solution of 15 mL ethanol, then 0.01 mol of cerium acetate hydrate (Sigma-Aldrich) and 0.001 mol citric acid monohydrate (C<sub>6</sub>H<sub>8</sub>O<sub>7</sub>·H<sub>2</sub>O,

SCRC) dissolved in 5 mL deionized water were added. The mixture was stirred for 2 h to ensure thorough mixing, and subsequently dispersed with a micropipette onto Petri dishes (100 mm in diameter), and was then placed in an oven to form a gel at 40 °C. After 48 h aging, the gel was dried at 80 °C for 24 h. Calcination was carried out by slowly increasing temperature from room temperature to 400 °C at 2 °C/min ramping rate and kept at 400 °C for 5 h.

## 2.2 Preparation of silver-supported mesoporous CeO<sub>2</sub>

Silver-supported mesoporous CeO<sub>2</sub> material was prepared by a modified ethylene glycol(EG) reduction route. 0.5 g mesoporous CeO<sub>2</sub> was dispersed in 100 mL of EG to form a mixture in a three-necked flask. Then a given amount of PVP (Sigma-Aldrich,  $M_r=29000$ ) and Ag(NO<sub>3</sub>)<sub>3</sub> (the molar ratio of PVP to Ag<sup>+</sup> was 5:1) were added. The flask was sealed and then pure N<sub>2</sub> was insufflated to replace the air. Subsequently, such a mixture was stirred and maintained at a refluxing temperature of 80 °C for 10 h in the dark. After cooling to room temperature, the mixture was filtrated, washed copiously with water and ethanol and dried under vacuum at 60 °C for 12 h then calcined at 300 °C for 5 h.

## 2.3 Antibacterial property measurement

To make a suspension, sterilized CeO<sub>2</sub> (500 mg) powder was added into 100 mL sterile water with mild sonication, and sterilized pure mesoporous CeO<sub>2</sub>, 1% Ag/CeO<sub>2</sub>, 3% Ag/CeO<sub>2</sub>, 5% Ag/CeO<sub>2</sub> powders (500 mg) were separately added into 100 mL sterilized water with mild sonication. The standard gram-negative bacteria *E. coli* (ATCC 25922) was inoculated into lactose broth (LB) and cultured aerobically at 37 °C for 24 h. Then 1mL aliquots of bacterial inocula were added into four 12 cm-diameter LB agar Petri-dishes, followed by the addition of four kinds of 3 mL CeO<sub>2</sub> powder suspension prepared hereinbefore to four Petri-dishes. The mixed suspension was put horizontally in the dish and cultured at 37 °C for 48 h. The growth of the bacterium on the dishes was observed by counting the number of colony.

## 2.4 Material characterization

The crystal structures of the samples were determined by a powder X-ray diffraction on a Rigaku D/max-RB diffractometer using Cu K<sub>α</sub> radiation ( $\lambda=0.15406$  nm). The XRD data were recorded for  $2\theta$  values between 10° and 80° with a 0.02° step size. Transmission electron microscopy (TEM) and energy-dispersive spectrometry (EDS) were taken for morphology and chemical composition by JEOL JEM-2010 transmission electron microscope, which was operated at 200 kV. The textural properties and porosity

of samples were studied by adsorption of nitrogen at 77 K with a Micromeritics ASAP-2010C instrument. Surface areas were calculated by the BET method and pore size distribution was analyzed using the BJH method.

## 3 Results and discussion

The XRD patterns of mesoporous CeO<sub>2</sub> and silver-supported mesoporous CeO<sub>2</sub> are illustrated in Fig. 1. The diffraction peaks at  $2\theta=28.5^\circ$ ,  $33.0^\circ$ ,  $47.4^\circ$  and  $56.4^\circ$  can be indexed to a cubic structure (space group *Fm3m*, JCPD NO43—1002)with lattice space  $a=0.541$  nm. The XRD patterns of 1%, 3%, 5% Ag-supported mesoporous CeO<sub>2</sub>, show only discernable diffraction peaks at  $2\theta=38.1^\circ$ ,  $44.3^\circ$ , which could be assigned to the metal silver(JCPD NO65—2871). The EDS spectrum in Fig. 2 shows 3% Ag-supported mesoporous CeO<sub>2</sub>, suggesting that only Ce, O and Ag are detected.

Figures 3(a), (b) show the TEM images of 3% Ag-supported mesoporous CeO<sub>2</sub>. The figures reveal that the sample is not organized [14] as well as that in the case of

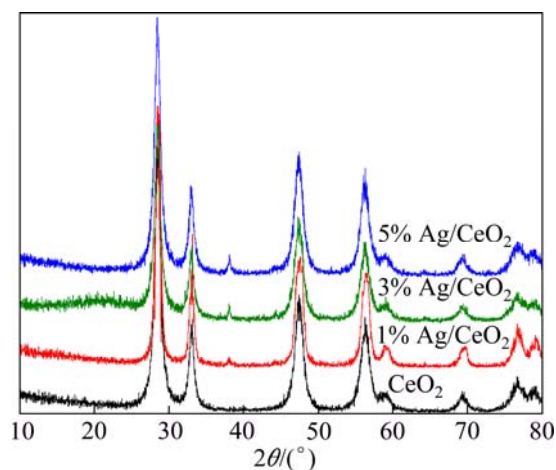


Fig. 1 XRD patterns of mesoporous CeO<sub>2</sub> and silver-supported mesoporous CeO<sub>2</sub>

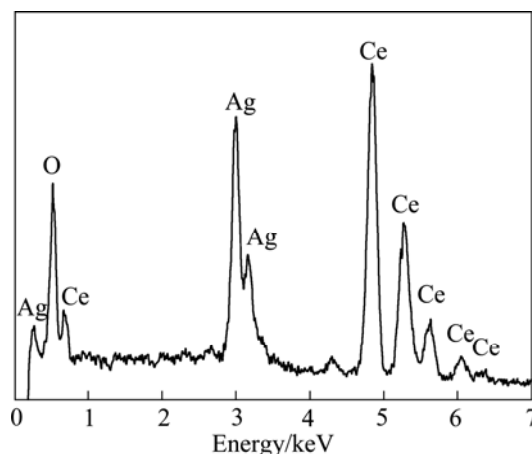
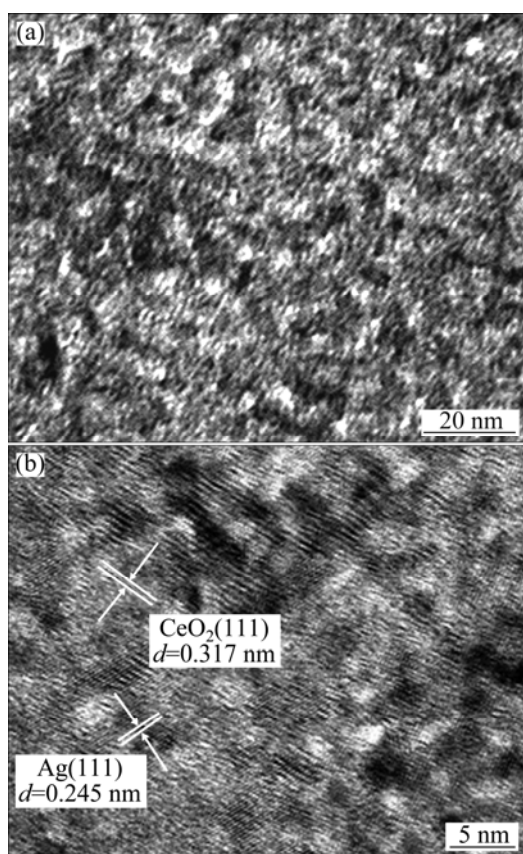


Fig. 2 EDS patterns of 3% Ag-supported mesoporous CeO<sub>2</sub>



**Fig. 3** TEM images of 3% Ag-supported mesoporous CeO<sub>2</sub>

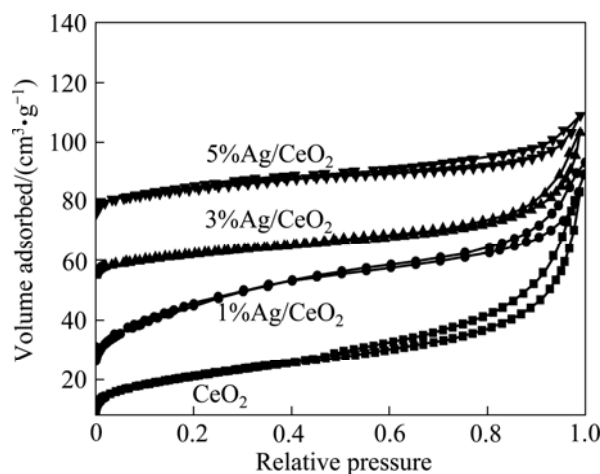
CeO<sub>2</sub> and consists of porous with diameter of 5–10 nm. The Ag nanoparticles are encapsulated by CeO<sub>2</sub> meso-structure and randomly distributed throughout the entire mesoporous CeO<sub>2</sub> framework. The CeO<sub>2</sub> meso-structure avoids a severe breakdown throughout the Ag nanoparticles supporting step. In Fig. 3(b), many different lattice fringes can be found which allows for identification of the crystallographic spacings of CeO<sub>2</sub> and Ag. The fringes of *d*0.317 nm match the (111) crystallographic planes of CeO<sub>2</sub>, while the fringes of *d*0.245 nm match the (111) planes of the metal Ag.

With CTAB as a surfactant and citric acid as a complexing agent, the mesostructure of CeO<sub>2</sub> was fabricated by the evaporation-induced self-assembly (EISA) process. After Ag(NO<sub>3</sub>) and PVP were added to the mesoporous CeO<sub>2</sub> ethylene glycol solution, on the pore of mesoporous CeO<sub>2</sub>, Ag<sup>+</sup> precursors were reduced with ethylene glycol to form silver atoms, then these silver atoms nucleated and grew into silver nanostructures. The whole reaction can be described by the following equations:

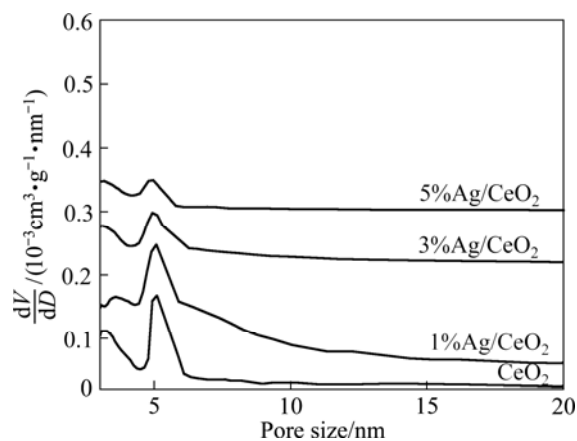


Figure 4 shows the nitrogen adsorption-desorption

isotherms of the mesoporous CeO<sub>2</sub> and Ag-supported mesoporous CeO<sub>2</sub>. According to IUPAC classification, the similar nitrogen adsorption-desorption isotherms of all samples can be classified as a type IV isotherm, and each hysteresis loop is H<sub>2</sub> type, typical of a mesoporous material. The nitrogen adsorption-desorption measurements of the mesoporous CeO<sub>2</sub> and Ag-supported mesoporous CeO<sub>2</sub> show a similar isotherm with a jump at a relative pressure of 0.3–0.5 that corresponds to the capillary condensation of the mesoporous and another jump at a relative pressure of 0.8–0.9, reflecting the textural pores between the particles. The pore size distributions are shown in Fig. 5, and the pore size of the samples is 5–7 nm. The BET specific surface area of the sample is summarized in Table 1. With the silver loaded amount increasing, the pore size and the BET specific surface area all decrease. This means that the Ag nanoparticles have incorporated into the pores of the mesoporous CeO<sub>2</sub>.



**Fig. 4** Nitrogen adsorption-desorption isotherms of mesoporous CeO<sub>2</sub> and Ag-supported mesoporous CeO<sub>2</sub>



**Fig. 5** Pore size distribution of mesoporous CeO<sub>2</sub> and Ag-supported mesoporous CeO<sub>2</sub>

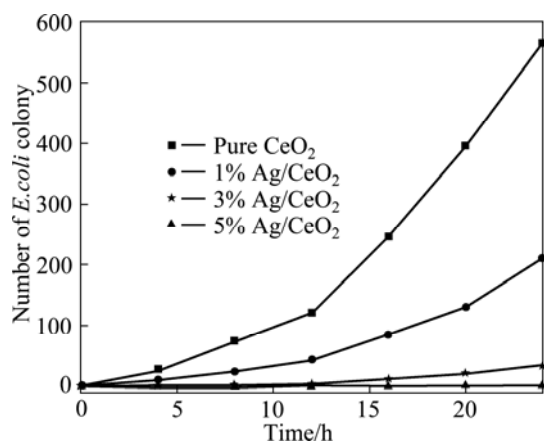
**Table 1** BET specific surface area of mesoporous CeO<sub>2</sub> and Ag-supported mesoporous CeO<sub>2</sub>

| Sample                 | BET specific surface area/(m <sup>2</sup> ·g <sup>-1</sup> ) |
|------------------------|--|
| CeO <sub>2</sub>       | 139  |
| 1% Ag/CeO <sub>2</sub> | 126  |
| 3% Ag/CeO <sub>2</sub> | 112  |
| 5% Ag/CeO <sub>2</sub> | 101  |

#### 4 Antibacterial activity

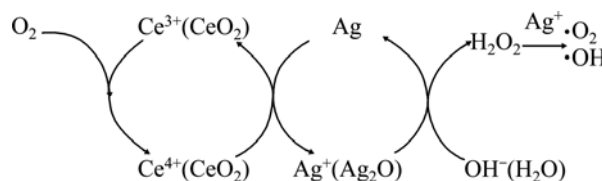
The mixed suspension was put horizontally in the dish and cultured at 37 °C for 48 h. The growth of the bacterium on the dishes was observed by counting the number of colony. The antimicrobial efficiency of the samples was tested against gram negative bacterium *E. coli*. Figure 6 shows four culture dishes with and without antibacterial agents after antibacterial test. In Fig. 6, no antibacterial activity was detected in the culture plate with pure mesoporous CeO<sub>2</sub> powder. After 24 h of the antibacterial test, the *E. coli* colonies number reached over 500. 48 h later, thick white lawn appeared on or around the dish. 1% Ag/CeO<sub>2</sub> shows little antibacterial activity because Ag<sup>+</sup> ions leading to inhibition of bacterium do not operate at such a low level of concentration.

Figure 6 shows that the antibacterial propriety of the suspension scattered on the dish is strong. The CeO<sub>2</sub> powders loaded with the silver nanoparticles significantly retard the bacteria growth. Ag nanoparticles have an appreciable effect on bacteria killing, as shown in Fig. 6 (3% Ag/CeO<sub>2</sub>), and the *E. coli* colony number does not exceed 50 after 24 h. This exhibits that Ag nanoparticles can endow CeO<sub>2</sub> powders with excellent antibacterial properties. Yet, the proportion of Ag doped in the materials is still inadequate. Therefore, a few colonies appear on the dishes. Figure 6 (5% Ag/CeO<sub>2</sub>) shows that the antibacterial propriety of the suspension

**Fig. 6** Antibacterial properties of pure mesoporous CeO<sub>2</sub> and Ag-supported mesoporous CeO<sub>2</sub> against *E. coli*

scattered on the dish is strong. The CeO<sub>2</sub> powders loaded with the silver nanoparticles (5%Ag/CeO<sub>2</sub>) entirely retard bacteria growth.

This good antibacterial activity is possibly due to Ag ions eluted from Ag-loaded mesoporous CeO<sub>2</sub> surface, which could be absorbed onto the surface of bacteria cells with damaging the cell membrane and solidifying structure of proteins structure. It will lead to a distortion of *E. coli* cell shape and give rise to leakage of the intracellular constituents, resulting in the death of the bacteria. The oxygen species released from the decomposition of Ag<sub>2</sub>O participated in the oxidation of hydroxide ion, and the reoxidation of Ag to Ag<sub>2</sub>O would be achieved via the oxygen species from mesoporous CeO<sub>2</sub>. Mesoporous CeO<sub>2</sub>, which possesses high surface area and well oxygen storage capacity, will interact with the oxygen molecules in the reaction stream through the cycle of Ce<sup>4+</sup>/Ce<sup>3+</sup> [23], maintaining the recycling of the oxidative state of the silver, as shown in Fig. 7. This excellent interface is thought to promote the formation of the reactive Ag ions. Based on this study it is possible to use this sort of powder as a promising bioactive antibacterial material.

**Fig. 7** Schematic illustration of oxygen transfer mechanism

#### 5 Conclusions

1) Mesoporous CeO<sub>2</sub> was synthesized using a modified evaporation-induced self-assembly method, different amounts of Ag were loaded on this mesoporous CeO<sub>2</sub> by a modified ethylene glycolreduction route. The obtained materials have a high surface area and uniform pore size.

2) When 5% Ag was loaded on the mesoporous CeO<sub>2</sub>, the antibacterial property shows that the sample has a considerable bactericidal activity, due to the synergistic effect between the silver nanoparticles and mesoporous CeO<sub>2</sub>.

#### References

- [1] MURUGAN B, RAMASWAMY A V. Defect-site promoted surface reorganization in nanocrystalline ceria for the low-temperature activation of ethylbenzene [J]. *J Am Chem Soc*, 2007, 129: 2062–2063.
- [2] ZHANG D S, PAN C S, SHI L Y, HUANG L, FANG J H, FU H X. A highly reactive catalyst for CO oxidation: CeO<sub>2</sub> nanotubes synthesized using carbon nanotubes as removable templates [J].

- Microporous Mesoporous Mater, 2009, 117: 193–200.
- [3] KOSYNKIN V D, ARZGATKINA A A, IVANOV E N, CHTOUTSA M G, GRABKO A I, KARDAPOLOV A V, SYSINA N A. The study of process production of polishing powder based on cerium dioxide [J]. *J Alloys Compd*, 2000, 303–304: 421–425.
- [4] HOSHINO T, KURATA Y, TERASKI Y, SUSAKI K. Mechanism of polishing of SiO<sub>2</sub> films by CeO<sub>2</sub> particles [J]. *Non-Cryst Solids*, 2001, 283: 129–136.
- [5] AVELLANEDA C O, BERTON M A C, BULHOESL O S. Optical and electrochemical properties of CeO<sub>2</sub> thin film prepared by an alkoxide route [J]. *Sol Energy Mater Sol Cells*, 2008, 92: 240–244.
- [6] PATSALAS P, LOGOTHETIDIS S, METAXA C. Optical performance of nanocrystalline transparent ceria films [J]. *Appl Phys Lett*, 2002, 81: 466–468.
- [7] ÖZER N. Optical properties and electrochromic characterization of sol-gel deposited ceria films [J]. *Sol Energy Mater Sol Cells*, 2001, 68: 391–400.
- [8] IZU N, SHIN W, MURAYAMA N, KANZAKI S. Resistive oxygen gas sensors based on CeO<sub>2</sub> fine powder prepared using mist pyrolysis [J]. *Sens Actuators B*, 2002, 87(1): 95–98.
- [9] LAOSIRIPOJANA N, SANGTONGKITCHAROEN W, ASSABUMRUNGRAT S. Catalytic steam reforming of ethane and propane over CeO<sub>2</sub>-doped Ni/Al<sub>2</sub>O<sub>3</sub> at SOFC temperature: Improvement of resistance toward carbon formation by the redox property of doping CeO<sub>2</sub> [J]. *Fuel*, 2006, 85(3): 323–332.
- [10] SUN C W, XIE Z, XIA C R, LI H, CHEN L Q. Investigations of mesoporous CeO<sub>2</sub>-Ru as a reforming catalyst layer for solid oxide fuel cells [J]. *Electrochem Commun*, 2006, 8(5): 833–838.
- [11] HU C Q, ZHU Q S, JIANG Z, ZHANG Y Y, WANG Y. Preparation and formation mechanism of mesoporous CuO-CeO<sub>2</sub> mixed oxides with excellent catalytic performance for removal of VOCs [J]. *Microporous Mesoporous Mater*, 2008, 113(1–3): 427–434.
- [12] MAO C J, ZHAO Y X, QIU X F, ZHU J J, BURDA C. Synthesis, characterization and computational study of nitrogen-doped CeO<sub>2</sub> nanoparticles with visible-light activity [J]. *Phys Chem Chem Phys*, 2008, 10: 5633–5638.
- [13] CORMA A, ATIENZAR P, GARCLA H, CHANE-CHING J Y. Hierarchically mesostructured doped CeO<sub>2</sub> with potential for solar-cell use [J]. *Nat Mater*, 2004, 3: 394–397.
- [14] ROSSINYOL E, ARBIOL J, PEIRÓ F, CORNET A, MORANTE J R, TIAN B. Nanostructured metal oxides synthesized by hard template method for gas sensing applications [J]. *Sens Actuators B*, 2005, 109(1): 57–63.
- [15] BARRABÉS N, DAFINOV A, MEDINA F, SUEIRAS J E. Catalytic reduction of nitrates using Pt/CeO<sub>2</sub> catalysts in a continuous reactor [J]. *Catal Today*, 2010, 149(3–4): 341–347.
- [16] CAI W J, WANG F G, VAN V A C, PROVENDIER H, MIRODATOS C, SHEN W J. Autothermal reforming of ethanol for hydrogen production over an Rh/CeO<sub>2</sub> catalyst [J]. *Catal Today*, 2008, 138: 152–156.
- [17] HOSOKAWA S, KANAI H, UTANI K, TANIGUCHI Y, SAITO Y, IMAMURA S. State of Ru on CeO<sub>2</sub> and its catalytic activity in the wet oxidation of acetic acid [J]. *Appl Catal B*, 2003, 45(3): 181–187.
- [18] FU Q, SALTSBURG H, FLYTZANI S M. Active non-metallic Au and Pt species on ceria-based water-gas shift catalysts [J]. *Science*, 2003, 301: 935–939.
- [19] CARRETTIN S, CONCEPCION P, COMA A, LÓPEZ NIETO J M, PUNTES V F. Nanocrystalline CeO<sub>2</sub> increases the activity of Au for CO oxidation by two orders of magnitude [J]. *Angew Chem Int Ed*, 2004, 43: 2538–2540.
- [20] IMAMURA S, YAMADA H, UTANI K. Combustion activity of Ag/CeO<sub>2</sub> composite catalyst [J]. *Applied Catalysis A*, 2000, 192(2), 221–226.
- [21] TOP A, ÜLKÜ S. Silver, zinc, and copper exchange in a Na-clinoptilolite and resulting effect on antibacterial activity [J]. *Appl Clay Sci*, 2004, 27(1–2): 13–19.
- [22] RAVINDRA S, MURALI M Y, REDDY N N, RAJU K M. Fabrication of antibacterial cotton fibres loaded with silver nanoparticles via “green approach” [J]. *Colloids Surf A*, 2010, 367(1–3): 31–40.
- [23] TANG X F, CHEN J L, LI Y G, LI Y, XU Y D, SHEN W J. Complete oxidation of formaldehyde over Ag/MnO<sub>x</sub>-CeO<sub>2</sub> catalysts [J]. *Chem Eng J*, 2006, 118(1–2): 119–125.

## Ag/介孔 CeO<sub>2</sub> 纳米复合材料的合成、表征及抗菌性能

陆晓旺<sup>1,2</sup>, 钱君超<sup>3</sup>, 陈丰<sup>3</sup>, 李霞章<sup>1</sup>, 陈志刚<sup>4</sup>

1. 常州大学 材料科学与工程学院, 常州 213164;
2. 常州市先进金属材料重点实验室, 常州 213164;
3. 江苏大学 材料科学与工程学院, 镇江 212013;
4. 苏州科技学院 化学与生物工程学院, 苏州 215011

**摘要:** 利用改进的溶剂挥发诱导自组合法(EISA)制备高比表面积介孔 CeO<sub>2</sub>, 通过改进的乙二醇还原法, 在得到的介孔 CeO<sub>2</sub> 中负载上不同量的银。采用粉末 X 射线衍射(XRD)、透射电子显微镜(TEM)、能谱仪(EDS), N<sub>2</sub> 吸附-脱附法方法对产物进行表征。由 BJH 方程计算得到材料的孔径分布, 以 BET 法计算材料的比表面积。研究负载不同比例银纳米粒子的介孔 CeO<sub>2</sub> 的结构及其抗菌活性。实验表明所制备的新材料具有很好的抗菌性能。

**关键词:** CeO<sub>2</sub>; 介孔; 银纳米颗粒; 抗菌活性

(Edited by LI Xiang-qun)